Waves & Oscillations in the Solar Atmosphere:
Heating and Magneto-Seismology
Proceedings IAU Symposium No. 247, 2007
R. Erdélyi & C. A. Mendoza-Briceño, eds.

doi:10.1017/S174392130801483X

Influence of longitudinal structure in the fast modes of prominence threads

A. J. Díaz, R. Oliver and J. L. Ballester

Universitat de les Illes Balears, Palma de Mallorca, Spain
email: toni.diaz@uib.es

Abstract. Recent high-resolution observations have pointed out that prominences are made of small threads (also named fibrils) piled up to form the body of the prominence. These fine structures also seem to support their own oscillatory modes, while their effect on the global modes of the prominences are less certain. We study the effect of adding a smooth transition layer between the prominence material and the corona along the magnetic field line, since previous studies have considered a jump in density in this interface. Then we compare the results with previous models and check that these transition layers do not affect significantly the periods of the modes.

Keywords. waves, Sun: atmosphere, Sun: Corona, Sun: oscillations

1. Introduction

Oscillations in prominence threads (also known in the literature as fibrils) have been reported in observational papers, specially recently using high resolution (Lin 2004, Lin *et al.* 2005, Lin *et al.* 2007). The fine structure is composed of thin magnetic flux ropes oriented along the magnetic field. These studies have revealed that the threads may oscillate independently with their own periods, which range between 3 and 20 minutes, superimposed with movements of dense material and flows (Lin *et al.* 2005).

The first theoretical investigation of periodic prominence perturbations taking into account prominence fine structure was performed in a Cartesian geometry by Joarder *et al.* (1997). Díaz *et al.* (2001) corrected and extended these results, and in Díaz *et al.* (2002), Díaz *et al.* (2003) the model was studied in more detail with the addition of longitudinal propagation and cylindrical geometry. The most important conclusions extracted from these studies are that prominence threads support only a few modes of oscillation corresponding to the lowest frequencies. Also, high harmonics are not trapped inside thin structures, and the spatial structure of the fundamental (even and odd) kink modes is such that the velocity amplitude outside the thread takes significant values over large distances, *i.e.* the energy confinement of the thread is poor. As a consequence, threads oscillate in groups rather than individually.

On the other hand, the internal structure of the threads is assumed to consist in a region where the dense material is located in the magnetic dip of the magnetic field line that supports it, while the rest of the rope is filled with coronal plasma. A sketch of this model can be seen in Fig. 1. However, a slab profile is just an approximation to a realistic profile, which would be smooth, but with a narrow transition region between the dense material and the evacuated part. The inclusion of a smoothed profile in the direction across the magnetic field leads to coupling between modes and resonant absorption (see for example see Goossens *et al.* 2006 and references therein).

The aim of this study is to investigate the properties of the stationary modes of a thread which a smooth transition to the coronal material along the magnetic field lines. Recently

there have been a number of studies dealing with the effects of including structure along the field lines in coronal loops when line-tying boundary conditions in the photospheric surfaces are included (Nakariakov et el. (2000), Nakariakov & Ofman (2001), Lorna 2003, Mendoza-Briceño *et al.* 2004, Díaz *et al.* (2002), Díaz *et al.* (2004), Díaz *et al.* (2006), Andries *et al.* 2005a, Andries *et al.* 2005b, Donnelly *et al.* 2006, McEwan *et al.* 2006, Dymova & Ruderman 2006, Erdélyi & Verth (2007), Díaz *et al.* (2007), Verth *et al.* 2007). Some of the effects that arise are shifts in the periods and modification in the spatial structure of the modes. In oscillations of prominence threads, these effects are also present if we compare them with a homogeneous loop filled with prominence material, since the existence of a evacuated part of the loop in the footpoints is a type of structuring along the magnetic field. However, we are interested in studying the differences between models with a jump compared with models with smoothed variations of density.

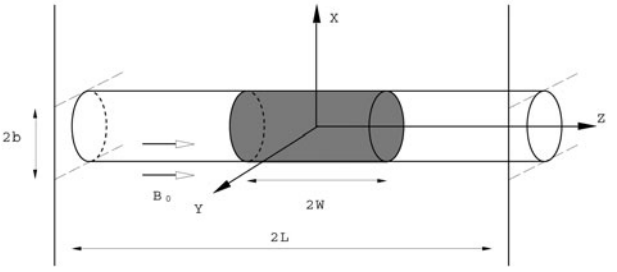

Figure 1. Sketch showing a simple equilibrium configuration for a prominence thread, which consists in a straight magnetic flux tube embedded in coronal plasma. The central part of the tube is filled with prominence material, while the rest of it is filled with coronal one. We are interested in studying a smooth transition along the magnetic field

2. Equilibrium model

Following the idea outlined above, we model a thread as a long flux tube with cylindrical geometry and line-tied to the photosphere at both sides. The flux tube has a length $2L$, which is believed to be much longer than the observed thread length, named $2W$. The tube has a radius a. The magnetic field $\mathbf{B_0} = B_0\mathbf{e_z}$ is assumed to be uniform throughout the medium and is aligned with the thread. The equilibrium density ρ_0 is structured both radially and longitudinally. Gravitational effects are ignored. We have included a sketch of this equilibrium configuration in Fig. 1.

Next is to choose a density profile that models a prominence thread. The most simple one is a slab profile with a dense density plateau in the center and a jump discontinuity at the thread limits $z = \pm W$:

$$\rho_0(0,z) = \begin{cases} \rho_\mathrm{p} & |z| \leqslant W \\ \rho_\mathrm{c} & W < |z| \leqslant L \end{cases} \tag{2.1}$$

This profile has the advantage of being amenable to an analytical solution, but numerically it is harder to solve directly, specially for finite differences methods. Therefore, it might be convenient to study also a smooth profile that resembles the slab, for example, one based on the Fermi-Dirac distribution:

$$\rho_0(0,z) = \rho_\mathrm{c}\left[1 + (\rho_\mathrm{p}/\rho_\mathrm{c} - 1)\frac{\exp\left[-W/\delta\right] + 1}{\exp\left[(|z| - W)/\delta\right] + 1}\right], \tag{2.2}$$

https://doi.org/10.1017/S174392130801483X Published online by Cambridge University Press

where δ is a measure of the transition region width. In the limit $\delta \to 0$ the slab profile in Eq. (2.1) is recovered, but for a finite δ the profile smoothly varies between the prominence and coronal region of the tube. These profiles have been represented in Fig. 2 for a range of transition region widths.

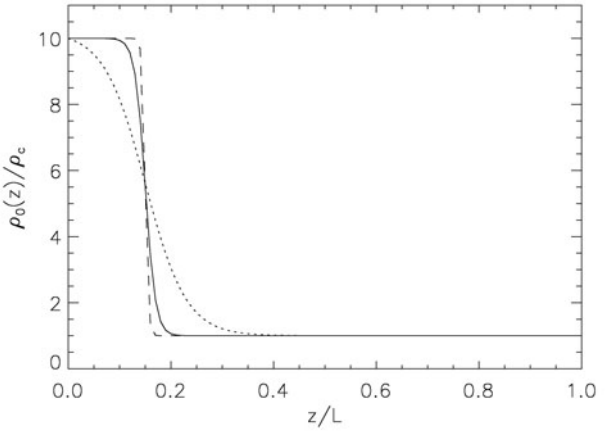

Figure 2. Density profiles along the magnetic field described by Eq. (2.2) for W/L=0.1 and $\rho_p/\rho_c = 10$. The dotted line has $\delta = 0.1$, the solid line $\delta = 0.05$ and the dashed line $\delta = 0.01$.

3. Wave equations

The ideal adiabatic MHD equations (neglecting gravitational effects) reduce to the following system of coupled partial differential equations Díaz *et al.* (2002):

$$\frac{\partial p_T}{\partial t} = \rho_0 c_A^2(z)\frac{\partial v_z}{\partial z} - \rho_0 c_f^2(z)\nabla\cdot\mathbf{v}\,, \tag{3.1}$$

$$\rho_0\left[\frac{\partial^2}{\partial t^2} - c_A^2(z)\frac{\partial^2}{\partial z^2}\right]\mathbf{v}_\perp = -\nabla_\perp\left[\frac{\partial p_T}{\partial t}\right], \tag{3.2}$$

$$\rho_0\left[\frac{\partial^2}{\partial t^2} - c_T^2(z)\frac{\partial^2}{\partial z^2}\right]v_z = -\frac{c_s^2(z)}{c_f^2(z)}\frac{\partial^2 p_T}{\partial z\partial t}\,, \tag{3.3}$$

where $c_A(z) = B_0/\sqrt{\mu\rho_0(z)}$ and $c_s(z) = \sqrt{\gamma P_0/\rho_0(z)}$ are the Alfvén and sound speeds, ${c_T}^{-2} = c_A^{-2} + {c_s}^{-2}$ determines the tube speed c_T, and $c_f^2 = c_A^2 + c_s^2$. The subscript '$\perp$' denotes components perpendicular to the equilibrium magnetic field, so the perturbed flow is $\mathbf{v} = \mathbf{v}_\perp + v_z\mathbf{e_z}$. The perturbed total pressure is p_T. Notice that in the derivation of these equations the magnetic field and gas pressure have been assumed to be constant in the z-direction, so the characteristic speeds depend only on the z-coordinate because of the equilibrium density $\rho_0(z)$. Eqs. (3.1)–(3.3) apply in each region of the flux tube and its environment.

The system of equations in Eqs. (3.1)–(3.3) are difficult to solve analytically. Therefore, we can gain a lot of information by exploring situations in which the MHD modes are decoupled. In prominence threads, the supporting magnetic arcade is long compared with the thread thickness, while under prominence conditions the plasma beta is $\beta \approx 10^{-2}$

https://doi.org/10.1017/S174392130801483X Published online by Cambridge University Press

(and $\beta \approx 10^{-3}$ in typical coronal conditions), making the low-beta plasma approximation quite accurate. Under these conditions we obtain from Eqs. (3.1)–(3.3) (Díaz *et al.* (2002))

$$\left[\frac{\partial^2}{\partial t^2} - c_{\rm A}^2(z)\nabla^2\right] p_{\rm T} = 0\,, \tag{3.4}$$

which must be solved together with Eq. (3.2) for obtaining the normal components of the perturbed velocity. This equation can be solved analytically (see Díaz *et al.* (2001), Díaz *et al.* (2002) for a more detailed discussion). This is done by using separation of variables in the form of

$$p_{\rm T}(r,\theta,z,t) = \sum_{s=0}^{\infty} u_s(r)\ \Phi(\varphi)\ h_s(z)\ e^{i\omega t}\,, \tag{3.5}$$

We can extract information about the fast mode oscillation by taking into account that the tube radius is much smaller than its length, that is $a \ll L$ (Dymova & Ruderman 2006). Thus, from Eq. (3.2) we obtain

$$\left[\frac{\partial^2}{\partial t^2} - c_{\rm k}^2(z)\frac{\partial^2}{\partial z^2}\right] \mathbf{v_r} = 0. \tag{3.6}$$

where $c_{\rm k}$ is the kink speed, defined as

$$c_{\rm k}\,(z) = \left[\frac{2B_0^2}{\mu\,(\rho_i\,(z) + \rho_e\,(z))}\right]^{1/2}, \tag{3.7}$$

in a tube with internal plasma density $\rho_i(z)$ and environment density $\rho_e(z)$.

It should be remarked that Eq. (3.7) is valid for the kink and fluting modes, but the sausage mode does not propagate in the thin tube limit, and therefore is not described by that equation. The remaining modes (kink and fluting) have very similar frequencies, so in this approximation their frequencies and z-dependent parts are the same.

4. Comparison between a smooth profile and a profile with a jump

We can solve Eq. (3.7) for the profiles in Eqs. (2.1) and (2.2). The solution for the slab profile can be obtained analytically, while the one for the smooth profile can be obtained with analytical approximations or by numerical methods.

First, we are interested in the properties of the modes for the slab profile in Eq. (2.1). The frequencies are represented in Fig. 3. It is interesting to notice the avoided crossings, similar to the results in Díaz *et al.* (2007) for coronal loops with structure along the field line, but in coronal loops the density enhancement is assumed to be near the footpoints, while in prominence threads the density enhancement is located at the top of the structure. Figure 3 can be compared with the plots in Díaz *et al.* (2002) for a thread with finite thickness, so we see that the frequencies are accurately reproduced with our approximations.

Next we solve Eq. (3.7) for the profile in Eqs. (2.2). Since we are interested in comparing the results with the slab profile, we choose a fixed width and density contrast between the thread and the corona and plot the effect of changing the smoothness of the profile varying δ. The result is represented in Fig. 4. We can see that when $\delta \to 0$ the results for a slab profile are recovered (Fig. 3). However, in the expected range of this parameter, which should be around 0.05 or less in prominence threads (since the transition seen in high-resolution images is sharp Lin 2004, Lin *et al.* 2005, Lin *et al.* 2007), the changes

https://doi.org/10.1017/S174392130801483X Published online by Cambridge University Press

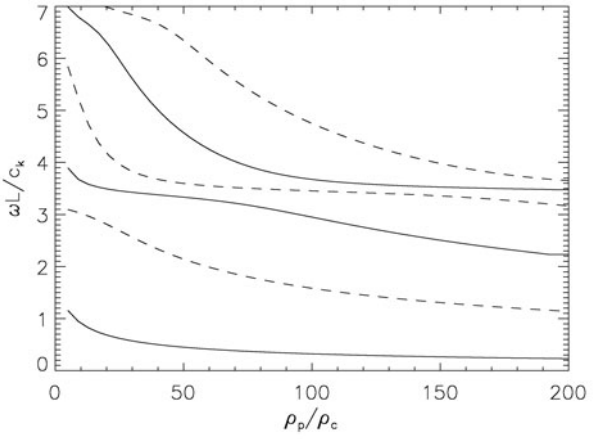

Figure 3. Solution to Eq. (3.7) for a slab profile of width $W/L = 0.1$ and density contrast $\rho_{\rm p}/\rho_{\rm c}$. Even modes are represented in solid lines, while odd modes are represented in dashed lines. Only the six lower modes have been plotted.

in the frequencies are small, specially compared with those produced by changing other parameters of the model, such as the thread width W or its density contrast with the corona.

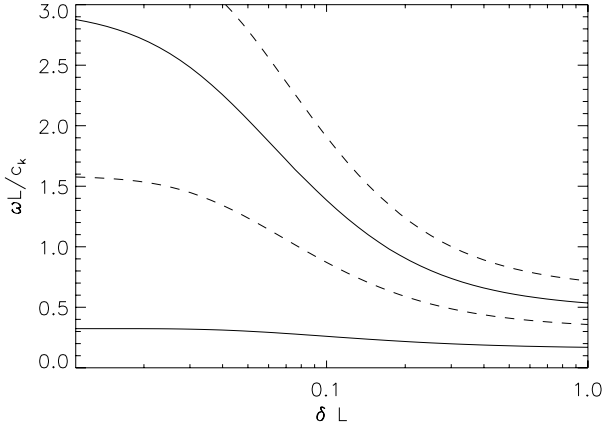

Figure 4. Numerical solution to Eq. (3.7) as a function of the transition layer thickness δ for the profile described in Eq. (4) of width $W/L = 0.1$ and density contrast $\rho_{\rm p}/\rho_{\rm c} = 100$. Even modes are represented in solid lines, while odd modes are represented in dashed lines. Only the four lower modes have been plotted.

5. Conclusions

We have studied the effect of a transition layer of thickness δ in the fast modes of a prominence thread. First of all, a differential equation was found for the fast kink modes using the low-beta plasma approximation and the fact that the thread width is much less than the length of the supporting magnetic arcade. With these assumptions the

https://doi.org/10.1017/S174392130801483X Published online by Cambridge University Press

fast mode is governed by Eq. (3.7), with no damping or coupling due to the addition of structuring.

Next we have compared the frequency of the modes of a smoothed profile with those with a jump discontinuity at the end of the thread dense region. This type of discontinuous models have been previously considered and their results match reasonably well with current observational reports of thread oscillations (Díaz *et al.* (2002)). We conclude that the addition of these transition layers does not affect significantly the frequencies and periods of the fast modes for the expected values of the layer thickness δ. Unfortunately, it is difficult to use as a tool for coronal seismology, since small variations in other parameters, such as the density contrast or the thickness of the thread, can outweigh the effect of the longitudinal structuring. Therefore, for more complicated studies, such as the introduction of a transition layer across the thread or the interaction of bunches of these threads, the effect of the longitudinal transition can be regarded as a secondary effect.

Acknowledgements

The authors acknowledge the financial support from the Spanish Government to support this research.

References

Andries, J., Arregui, I., & Goossens, M. 2005, Ap. J. L., 624, L57.
Andries, J., Goossens, M., Hollweg, J. V., Arregui, I., & Van Doorsselaere, T. 2005, A&A, 430, 1109.
Díaz, A. J., Oliver, R., Erdélyi, R., & Ballester, J. L. 2001, Ap. J., 580, 550.
Díaz, A. J., Oliver, R., & Ballester, J. L. 2002, Ap. J., 580, 550.
Díaz, A. J., Oliver, R., & Ballester, J. L. 2003, A&A, 402, 781.
Díaz, A. J., Oliver, R., Ballester, J. L., & Roberts, B. 2004, A&A, 424, 1055.
Díaz, A. J., Oliver, R., & Ballester, J. L. 2006, Ap. J., 645, 766.
Díaz, A. J., Donnelly, G. R.,& Roberts, B. 2007, A&A, 476, 359.
Donnelly, G. R., Díaz, A. J., & Roberts, B. 2006, A&A, 457, 707.
Dymova, M. V. & Ruderman, M. S., 2006, A&A, 457, 1059.
Erdélyi, R., & Verth, G. 2007, A&A, 462, 743.
Goossens, M., Andries, J., & Arregui, I. 2007, Phil. Roy. Soc. A, 364, 433.
Joarder, P. S., Nakariakov, V. M. & Roberts, B. 1997, Sol. Phys., 176, 285.
Lin, Y. 2004, PhD Thesis, Institute of Theoretical Astrophysics, Univ. of Oslo.
Lin, Y., Engvold, O., Rouppe van der Voort, L. H. M., Wiik, J. E., & Berger, T. E. 2005, Sol. Phys., 226, 239.
Lin, Y., Engvold, O., Rouppe van der Voort, L. H. M., & van Noort. 2007, Sol. Phys., 71.
James, L. 2003, Master Thesis, University of St Andrews.
McEwan, M. P., Donnelly, G. R., Díaz, A. J. & Roberts, B. 2006, A&A, 460, 893.
Mendoza-Briceño, C. A., Erdélyi, R., & Sigalotti, L. D. G. 2004, Ap. J., 605, 493.
Nakariakov, V. M. & Ofman, L. 2001, A&A, 372, L53.
Nakariakov, V. M., Verwichte, E., Berghmans, D. & Robbrecht, E. 2000, A&A, 362, 1151.
Verth, G., Van Doorsselaere, T., Erdélyi, R., & Goossens, M. 2007, A&A, 475, 341.